EXPERIMENTAL STUDY OF HALO FORMATION IN SPACE CHARGE DOMINATED BEAM*

H. D. Zhang#, B. L. Beaudoin, R. A. Kishek,
University of Maryland, College Park, MD 20742, USA

Abstract

Beam halos are a group of particles with low density that are far away from the well-defined central beam core and have large transverse velocities. Beam losses from halos can require a larger aperture and impose restrictions on the beam current. Several theoretical techniques have been applied to analyze and understand halo formation, including the particle-core model, the free energy model as well as particle in cell (PIC) simulations. However, few experiments on beam halos have been carried out. Here, we describe an experimental study at the University of Maryland to understand and characterize space-charge induced halo formation. The experiments are conducted on the University of Maryland Electron Beam (UMER) and the results are compared with PIC simulations using WARP.

INTRODUCTION

Halo is generally understood as a population of particles that do, or will reach large transverse radii relative to a more intense, centralized beam core. It is associated with emittance growth, degradation of beam quality and particle loss [1]. Several analytic models such as the particle-core model [2] and the free energy model [3] are derived either to depict the process of halo formation or to describe the associated emittance growth. Many theoretical and simulation studies developed these ideas and discussed various mechanisms for halo formation. However, fewer experimental studies have been performed as it is hard to obtain a halo free beam, a crucial component to identify different mechanisms or sources for halo formation. The LEDA experiment [4] is an example for demonstrating agreement with the particle-core model. But its propagation length is limited and it is no longer operational. In this paper, we discuss a method to get a halo-free beam though envelope match and skewness correction. Based on the matched beam, we perform a mismatch experiment as well as a skewness test to verify the sources of halo formation in UMER. Then, we generate a pure breathing mode mismatch, and compare experiments with simulations to confirm this mode.

EXPERIMENT SETUP

UMER

UMER [5], is small compact electron ring with a low energy (10 keV) but relatively high beam current (0.6-100 mA). It is designed to study the physics of electron beams from the emittance dominated regime to space charge dominated regime. The results can be scaled to higher energy beams with higher mass. Fig. 1 shows a schematic of the UMER layout, and Table 1 lists its key parameters and Table 2 lists the beam parameters we will use in this discussion.

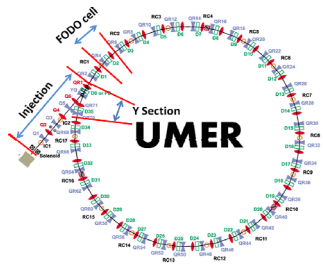

Figure 1: Diagram of UMER.

Table 1: UMER Design Parameters [5]

Parameter	Value
$\beta = v / c$	0.2
Pulse Length	20-120 ns
Beam Energy	10 keV
Current	0.6-100 mA
Ring Circumference	11.52 m
Lap Time	197 ns
Pulse Repetition Rate	10-60 Hz
FODO Period	0.32 m
Zero-current Phase Advance	0.760

Table 2: Beams in UMER [5]

Aperture#	r_0 (mm)	I (mA)	ε (μm)	χ
1	0.875	6	16.8	0.605
2	1.5	21	30.0	0.901

Image System

An imaging system was designed and dedicated for this work utilizing Ethernet cameras, in order to take and process images quickly. A system illustration is shown in Fig. 2. The cameras are connected to a control PC through a gigabyte Ethernet switch. The camera control PC can also control the magnets though the main control PC by sending an appropriate command. The whole system is integrated by a Matlab GUI code. It includes a camera control panel, Magnet control panel, image display and calculation panel, and the Auto picture scan panel. It allows one to change camera settings and take beam images, in order to calculate transverse beam parameters; such as centroid, size and rotation angle. This system can also be used for injection scan (empirical method discussed later) and phase space tomography.

*Work supported by the US Dept. of Energy, office of Science,
#haozhang@umd.edu

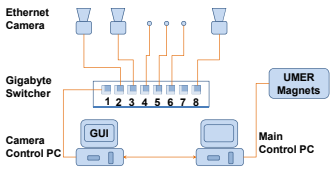

Figure 2: Illustration of imaging system.

ENVELOPE MATCH

Match Description and Fitting

We use a tracking code Trace3D to get a match solution. There are 3 different sections in UMER when we discuss beam envelope match, including injection, Y-section and ring section. Ring section contains 34 equivalent FODO cells, and the matched periodic envelope solution is defined by the emittance from Table 2 and the predefined lattice setting, specially the ring quadrupole strength. In UMER, the ring quadrupoles are setting to 659.0 G/m with positive and negative value alternating. Y-section contains a regular FODO cell, YQ and QR1, where the later two are pulsed Panofsky quadrupoles. Because the pipe for injection and recirculation go through YQ, the center line of YQ is off the ideal beam path by 10°, which results a slightly difference in peak gradient. We use Type 8 fitting procedure in Trace3D to find the quadrupoles setting for Y-section. Next step is to find appropriate injection quadrupole settings with the YQ and QR1 strength determined from last step. The lattice of injection starts from the aperture and ends at the entrance of a regular FODO cell. The final beam parameter is predefined by the ring FODO cell. Here, Q1 is usually small to avoid large ratio of two transverse sizes. The initial Twiss parameter at aperture is from Table 2. Using a Type 8 matching procedure in Trace3D, we will finally get a series of quadrupole setting either Q2-Q5 or Q3-Q6.

Empirical Matching

In practice, many factors, such as beam initial properties, lattices imperfection, vacuum condition and etc., will affect calculations and simulations, and make them deviate from experiments. The magnets strength obtained though calculation and simulation does not necessarily yield a good matching condition. A further empirical method will be used to achieve the final match. The idea here is to scan 4 injection quadrupoles and to take the envelope responses in more than 4 screens. The optimal solution can be obtained in a least square sense, i.e. $\Delta I = (R^{T}R)^{-1}R^{T}E$, where ΔI is the difference between current and updated quadrupole setting, R is response metrix, E is the envelope of current settings. An updated injection setting is given by I-ΔI. Details for this method can be referred to [6].

Correction for Skewness

Due to fringe field of solenoid and rotation error of injection quadrupoles, there is a beam rotation in each chamber inside the ring which also can be a source for halo formation. Here we use two skew quadrupoles in Q3 and Q6 to correct this rotation. The skew quadrupole is a type of UMER quadrupole with a normal pair of printed-circuits [6] and a 45-degree rotated pair as in Fig. 3. Each pair is powered by different current supplies, so the normal and skew components can be independently adjust. By scanning the skew quadrupoles and comparing the rotation angle of beam images in each chamber, we can minimize the rotation in least square sense similarly to the empirical matching.

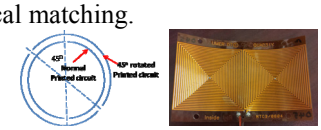

Figure 3: Schematic diagram of skew quadrupole (a) and piece of printed circuit (b).

Matching Result

After going through the process mention above, we obtain match beams of 6mA and 21 mA. The image of the beam for the first turn is shown in Fig. 4. The beam sizes in each chamber are plotted in Fig. 5. Note that, the screen is 28.6 mm ahead of ring chamber center and we also have a small difference of edge focusing in two transverse directions from dipole. Therefore, beam images in the screen are not round. Here, we calculate the average sizes are 3.55 mm, 2.79 mm for 6mA and 6.00 mm, 4.81 mm for 21mA and the standard derivations are 0.17 mm, 0.16 mm for 6mA and 0.30 mm, 0.17 mm for 21mA, which proof that we match the beam quite well. Meanwhile, the rotation angle is small, the average and standard derivation of which is only 0.4 degree and 8.3 degree for 6mA, and -1.4 degree and 7.7 degree for 6mA.

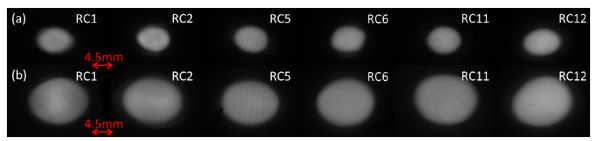

Figure 4: Matched beam images at different ring chamber: (a) 6mA; (b) 21mA.

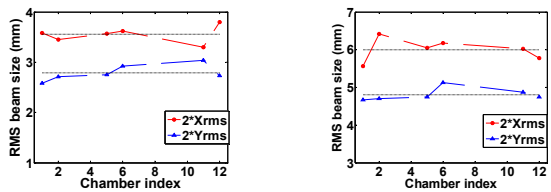

Figure 5: Plot of matched beam size 6mA (left); 21mA (right).

MISMATCH EXPERIMENT

Halo Related to Mismatch and Skewness

From the matched 6 mA beam, we mismatch the beam simple by reduce one of the quadrupole in the injection, e.g., Q5 by 20%, which is a huge error in realistic sense. We compared the beam images in RC5 between matched and mismatched case in Fig. 6. The phase space x-x' plot and y-y' plot is from phase space tomography. From the configuration space, it is clear that there are large amount of halo generated due to mismatch. From the phase space plot, there are also two hot spots in x-x' plot and large

spikes in y-y' plot, which indicate an emittance growth related to that halo.

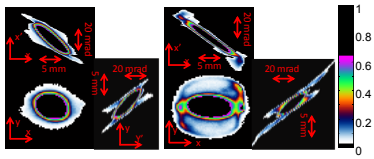

Figure 6: Comparison of matched (left) and mismatched (right) beam at RC5 in x-y, x-x', y-y' plots.

Beam rotation is also a driving source for halo formation. In order to see the halo generated in first turn, we intentionally introduce a 22.3° rotation in RC1 by setting the skew component of Q6 by 0.4 A (or 144.4 G/m peak gradient). The beam images are shown in Fig. 7. It is obvious from images in RC1 to RC5 that there is a wobbling mode related to beam rotation. When the beam finally gets close to equilibrium state (see in RC11 and RC12), the wobbling energy will be transfer to particles to form halo.

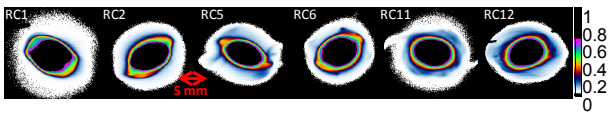

Figure 7: Halo generation from the rotation of the beam.

Pure Breathing Mode Generation

To generate quadrupole solutions that produce a pure breathing mode mismatch beam, we need to go back to the matched ellipse parameters at a little downstream of the screen in RC1, where two *beta functions* are equal. A breathing mode mismatch solution is obtained by scaling α_x, β_x, α_y and β_y there by a common factor μ^2, where μ is the mismatch parameter. From previous aperture condition and lattice settings in Trace3D, we change the setting of the final condition as the scaled twiss parameters, use a Type 8 matching procedure, and we can find the settings of quadrupole Q2-Q5, or Q3-Q6.

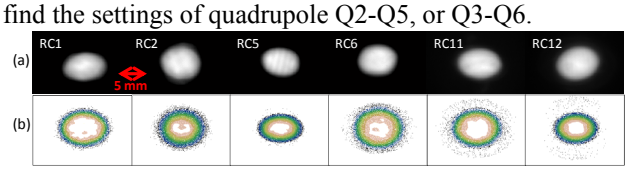

Figure 8: Breathing mode mismatch comparison between (a) experiment and (b) WARP simulation with mismatch parameter μ=1.3.

Here is an example of breathing mode mismatch using 6mA beam in Fig. 8 (a) where the mismatch parameter μ=1.3. Since the screen is offset from the center of each chamber, the breathing of beam envelope is not obvious from the images. To testify the mode we generate, we perform a PIC simulation using Warp [7]. The same emittance and current of 6mA beam are used and the breathing mismatch mode is generated the same way by scaling the α_x, β_x, α_y and β_y by a common factor μ^2 at the point when two *beta functions* are equal. The difference in simulation is we only use the ring section instead of starting from the aperture. The simulated images are shown in Fig. 8 (b). We plot the envelopes of this mismatched beam in Fig. 9 with dotted line from simulation and red dot representing the experimental data from each screen. From the plots, the experimental data lie on the simulation curve quite well which confirms a good agreement.

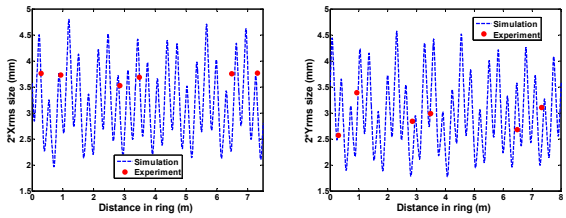

Figure 9: Envelope of the breathing mode mismatch: x (left) and y (right).

Next, we perform a FFT analysis to the envelope curves of breathing mode mismatch from simulation (see Fig. 10). We got a single strong peak for each direction with peak wave number 5.561 m^{-1} and 5.561 m^{-1} separately. This wave number is close to the result from analytic model 5.775 m^{-1}, which verifies that we generate a pure breathing mode.

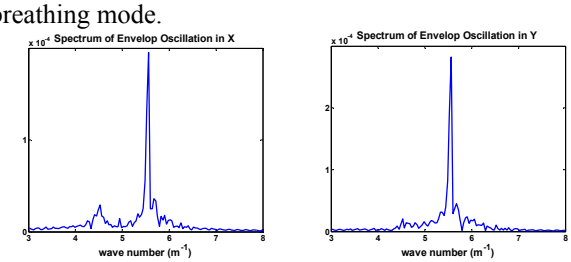

Figure 10: FFT analysis of the envelope for breathing mode mismatch: x (left) and y (right).

CONCLUSION

In this paper, we discussed a method in UMER for beam match which can be performed generally in any accelerator. We identified the sources for halo formation in UMER are from envelope mismatch and beam rotation. We generated a pure breathing mismatch mode in UMER and verified it. The pure mismatch mode has simpler dynamics, which will allow us study the halo formation related to mismatch quantitively. For near future, we will continue to study the breathing mode mismatch, especially compare beams in different space charge region.

REFERENCES

[1] A.V. Fedotov, et.al. *Proc. European Part. Acc. Conf.*, Vienna, p. 1289 (2000).
[2] R. Gluckstern. *Phys. Rev. Lett.*, 73 (1994).
[3] M. Reiser. *Journal of Applied Physics*, 70 (1991).
[4] C. K. Allen, et.al. *Phys. Rev. Lett.* 89, 214802 (2002).
[5] R.A. Kishek, et al., *R.A. Kishek, et al., Nuclear Instruments & Methods in Physics Research A,* in Press (2013).
[6] H. Li, Control and Transport of Intense Electron Beams, *Ph.D. Dissertation*, Univ. of Maryland, 2004.
[7] D.P. Grote, et al. *Nucl. Instr. and Meth. A*, vol. 415, p. 428 (1998).